On the Nonuniformity in Fluidized Bed

By

Mitsuhiro FUKUDA*, Zenjiro ASAKI* and Yoshio KONDO*

(Received March 29, 1967)

Mean (μ_c) and variance (σ_c^2) of local particle concentration in fluidized bed were measured by capacitance probe method using integrator and vacuum tube thermocouple. Particle concentration in bubble and dense phases (c_b and c_d), rise velocity of bubble (u_b), bubble thickness (y) and its frequency (f) were also measured from the signal current recorded on oscillograms.

The effects of fluidizing conditions on μ_c and σ_c^2 were studied. In the bulk of bed, μ_c remains at a value fixed by the fluidizing conditions. It decreases with air velocity. σ_c^2, on the other hand, increases with probe level up to considerably higher portion of bed and there arrives at a constant value which increases with bed height and air velocity.

The following equation was introduced to represent μ_c by the fluidizing characteristics.

$$\mu_c=\frac{yf}{u_b}c_b+\left(1-\frac{yf}{u_b}\right)c_d$$

μ_c calculated by this equation coincides well with the measured μ_c. A regression equation of σ_c^2 upon fluidizing characteristics,

$$\sigma_c^2=0.72\left\{\frac{yf}{u_b}\left(1-\frac{yf}{u_b}\right)\right\}^{0.46}(c_d-c_b)^{2.89}$$

was obtained, and the statistical analyses on this equation revealed that σ_c^2 changes chiefly with (c_d-c_b), and accordingly, σ_c^2 represents the nonuniformity in fluidized bed mainly in the form of particle concentration difference between bubble and dense phases.

1. Introduction

It is clarified by many works[1),2)] contributed to the gas fluidized bed that the bulk of excess gas stream above its minimal fluidization passes through the bed in the form of bubbles and that the fluidized bed is composed of two phases, bubble and dense phases. This nonuniformity of fluidized bed affects the rate and mechanism of heat- and mass-transfer and chemical reactions occuring in the bed, and many of the recent works were directed to study on the behaviror of bubbles, such as their size, rise velocity and frequency, particle concentration in bubble and dense phases and cross-flow of gas and solid particles between the two phases.[1),3),4),5)]

* Department of Metallurgy.

On the other hand, some of the earlier works pursued the correlationship between nonuniformity of fluidized bed and the fluidizing conditions, such as particle size and its distribution, bed height and flow rate of gas. Different uniformity indices were proposed by different workers.[6),7)] Dotson[8)] examined the effects of various fluidizing conditions on his uniformity index using statistically designed experiments. However, these uniformity indices introduced are thought troublesome because of their way of calculation in which a large amount of data should be treated using planimeters. Moreover, characteristics of their indices are supposed to be rather ambiguous.

These two ways of approach to the nonuniformity of fluidized bed, one through the behavior of bubbles and the other through the nonuniformity idisces, are thought better combined together, because of the indispensable role of nonuniformity on grasping the gas fluidized bed as a whole.

The local particle concentration in fluidized bed varies with time and it can be represented by two measures, mean and variance. The latter measure of particle concentration is proposed to represent the nonuniformity of fluidized bed. It is intended in this work, therefore, to measure the mean and variance of local particle concentration in fluidized bed, and to correlate them with the fluidizing conditions of bed height and flow rate of gas. Efforts are also directed to combine these measures with fluidizing characteristics which include the size, rise velocity and frequency of bubbles and also the particle concentration in bubble and dense phases in fluidized bed.

2. Experimental

2.1 Apparatus

Fig. 1 demonstrates a schematic illustration of the fluidizing apparatus. The fluidization column was made of 106 mm. I.D. and 1218 mm. long transparent Panlite resin tube. The distributor consists of a 300-mesh brass screen sandwitched between two 1.0 mm. thick aluminum plates perforated with 1.0 mm. D. holes spaced on a 7.0 mm. triangular pitch. The flow rate of air is metered through rotameters or through an orifice meter.

Details of capacitance probes are shown in Fig. 2. The tips of lower and upper probes were designed to separate each other by 24 mm. The tips are essentially an 1.5 mm. D. brass wire condenser and their cross-sectional area are sufficiently small so as to minimize the disruption of bed in the vicinity. By means of oscillator and detector curcuit shown in Fig. 3, the changes of capacitance of the probes are linearly converted into D.C. signals and their traces on a 2-channel

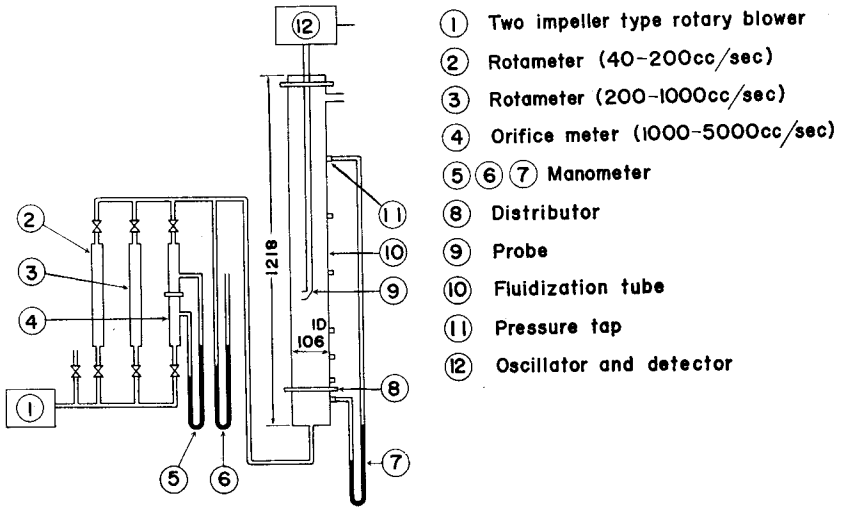

Fig. 1. Apparatus.

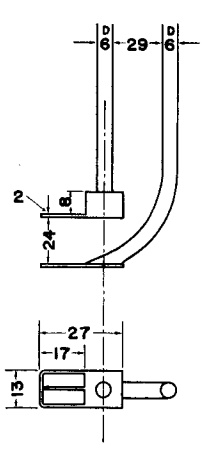

Fig. 2. Tips of capacitance probe.

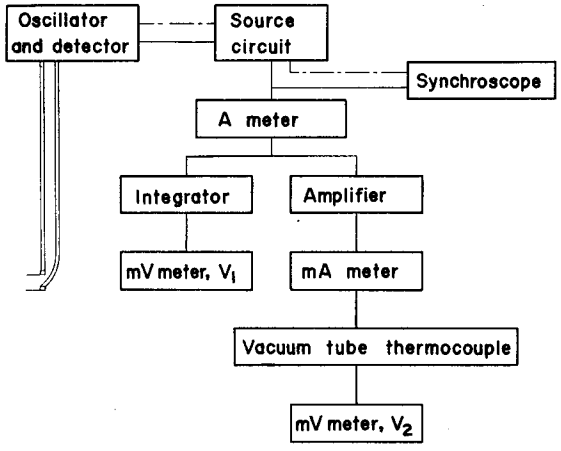

Fig. 3. Block diagram of circuit.

synchroscope are filmed three times in a 30 seconds interval. The scanning speed of the synchroscope was chosen at 0.1 second per cm. The scanning speed of 0.5 second per cm. was also employed for counting the frequency of bubbles. The D.C. signals are also transmitted to an integrator and a vacuum tube thermocouple to measure their mean and variance, respectively. The time constant of the integrator was chosen at 10 seconds.

2.2 Materials

Two different size spherical glass beads were used as fluidized material throughout the study. Most of the measurements were performed on the glass beads whose size distribution and physical properties are summarized in Fig. 4(A). The size distribution of another glass beads is illustrated in Fig. 4(B).

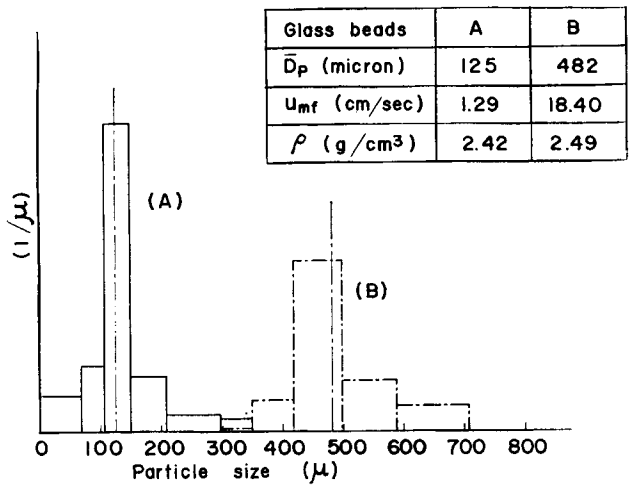

Fig. 4. Size distribution and physical properties of glass beads.

2.3 Fluidizing characteristics

Mean (μ_v) and variance (σ_v^2) of the D.C. signal (v) are defined by the following equations.

$$\mu_v=\frac{1}{\theta}\int_0^\theta v d\theta \tag{1}$$

$$\sigma_v^2=\frac{1}{\theta}\int_0^\theta (v-\mu_v)^2 d\theta$$

$$=\frac{1}{\theta}\int_0^\theta v^2 d\theta-\mu_v^2 \tag{2}$$

μ_v of Eq. (1) is obtained as output voltage from the integrator, v_1. The first term on the right side of Eq. (2) is obtained as output v_2 from the vacuum tube thermocouple. Mean (μ_c) and variance (σ_c^2) of particle concentration in non-dimensional form are calculated as μ_v and σ_v^2 divided by μ_s and μ_s^2, respectively;

$$\mu_c=\frac{\mu_v}{\mu_s} \tag{3}$$

$$\sigma_c^2=\frac{\sigma_v^2}{\mu_s^2} \tag{4}$$

μ_s is output voltage from the integrator at zero air velocity.

An example of oscillogram of the signal is shown in Fig. 5. Interpretation of these oscillograms offers the fluidizing characteristics such as size, rise velocity and frequency of bubbles, and particle concentration in dense and bubble phases.

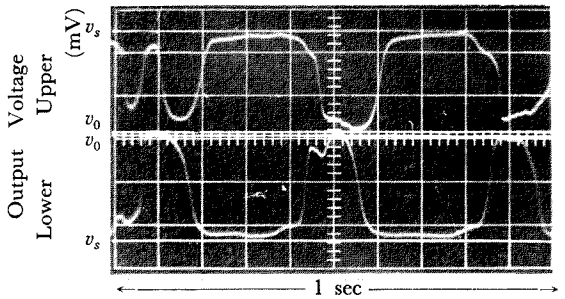

Glass beads: A, u=11.34 (cm/sec)
L_c/D_T=2.5 (−), Probe height=27 (cm)

Fig. 5. An example of oscillogram.

Particle concentration in bubble phase in nondimensional form, c_b, is obtained from the average peak height (v_b) on the oscillogram, by,

$$c_b=\frac{v_b-v_0}{v_s-v_0} \tag{5}$$

where v_0 and v_s are the height of traces filmed on empty column and on settled bed, respectively. Nondimensional particle concentration in dense phase, c_d, is calculated from average valley height (v_d), as,

$$c_d=\frac{v_d-v_0}{v_s-v_0} \tag{6}$$

Rise velocity of bubbles (u_b) is represented by the ratio of distance between lower and upper probes, 24 mm., to average time lag of signal waves on the oscillogram. The width of signal wave provides the passing time of bubbles through the probe tip. The average thickness of bubbles in vertical direction (y) is calculated by the average width of signal waves (δ) and the rise velocity of bubbles, as,

$$y=\delta u_b \tag{7}$$

The frequency of bubbles (f) is determined by counting the number of signal waves and dividing them by the time elapsed.

2.4 Experimental allocation

The bed height and flow rate of air were chosen as the independent factors. The combinations of their levels are listed in Table 1. Effects of particle size were also tested partially.

Tabel 1. The factors and their levels at which experiments are carried out.

Glass beads A	($\bar{D}_p=125\,\mu$, $u_{mf}=1.29$ cm/sec)
	Relative bed height, $L_c/D_T=1.0$, 2.5, 4.0 (−)
	Air velocity, $u=1.70$, 3.40, 5.67, 11.34, 20.86, 28.91, 40.14 (cm/sec)
Glass beads B	($\bar{D}_p=482\,\mu$, $u_{mf}=18.40$ cm/sec)
	Relative bed height, $L_c/D_T=2.0$, 3.0 (−)
	Air velocity, $u=22.68$, 27.44, 31.75, 43.65 (cm/sec)

3. Results

3.1 Mean and variance of particle concentration

Mean (μ_c) and variance (σ_c^2) of particle concentration in a fluidized bed of $L_c/D_T=4.0$ and $u=40.14$ cm/sec are illustrated in Fig. 6. Examining this and many other similar illustrations indicates the following;

μ_c:

1) μ_c around the central axis of bed is lower than those in the vicinity of column wall.

2) In the lower part of bed, μ_c increases in raising probe level towards its maximal value and it decreases slightly or remains unvaried in the upper part.

σ_c^2:

1) σ_c^2 around the central axis is higher than those near the column wall.

2) σ_c^2 increases with the probe level up to considerably higher portion and it varies scarcely there.

Thus, it may be said that the bubbles tend to rise around the central part of bed and that the fluidized particles are floating above the distributor because of low μ_c at the bottom of bed. Though μ_c and σ_c^2 vary at the bottom of fluidizing column, their variations become so slight in the upper part of bed and their means, $\overline{\mu}_{cm}$ and $\bar{\sigma}_{cm}^2$ in this part are thought to represent the fluidization itself. They will be discussed hereafter. Fig. 7 illustrates the relationship between $\overline{\mu}_{cm}$ and the excess superficial air velocity ($u-u_{mf}$). It is seen in this figure that the effect of L_c/D_T and D_p are scarcely followable and that $\overline{\mu}_{cm}$ of the fluidized bed are determined chiefly by ($u-u_{mf}$).

Similarly, Fig. 8 represents the effects of ($u-u_{mf}$) upon $\bar{\sigma}_{cm}^2$. Measuring

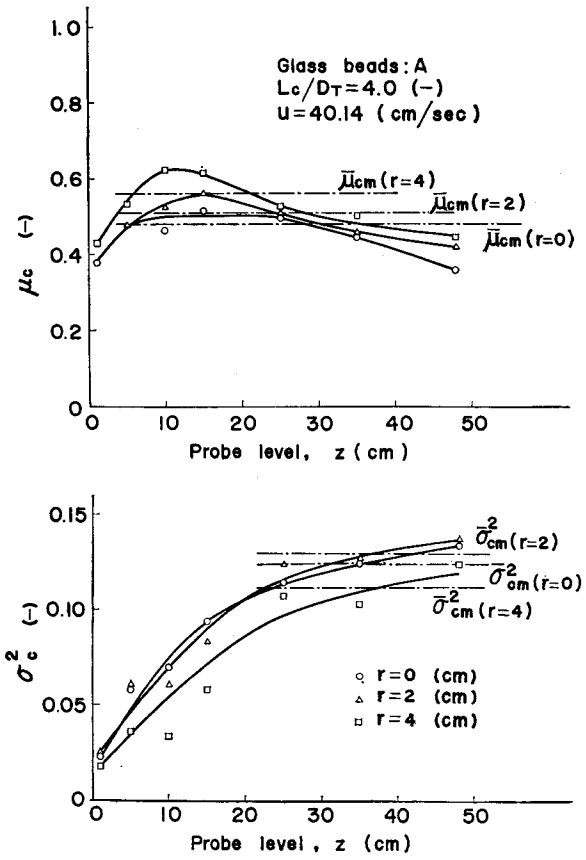

Fig. 6. An example of mean and variance of particle concentrations.

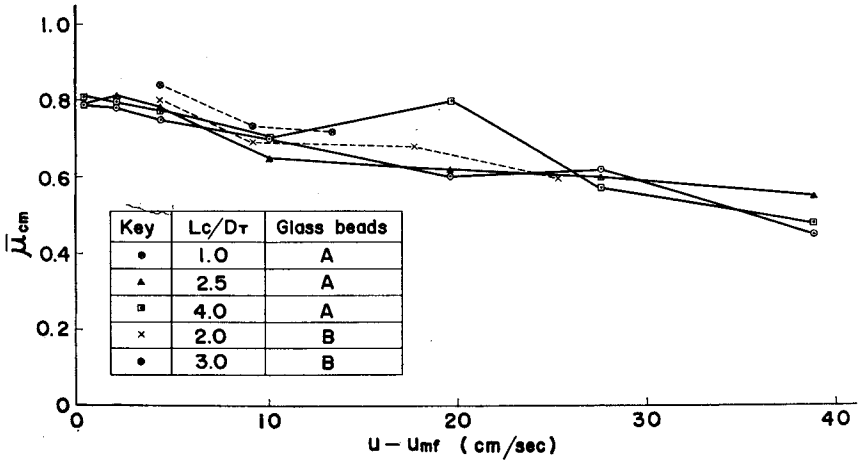

Fig. 7. Effect of excess air velocity on $\bar{\mu}_{cm}$.

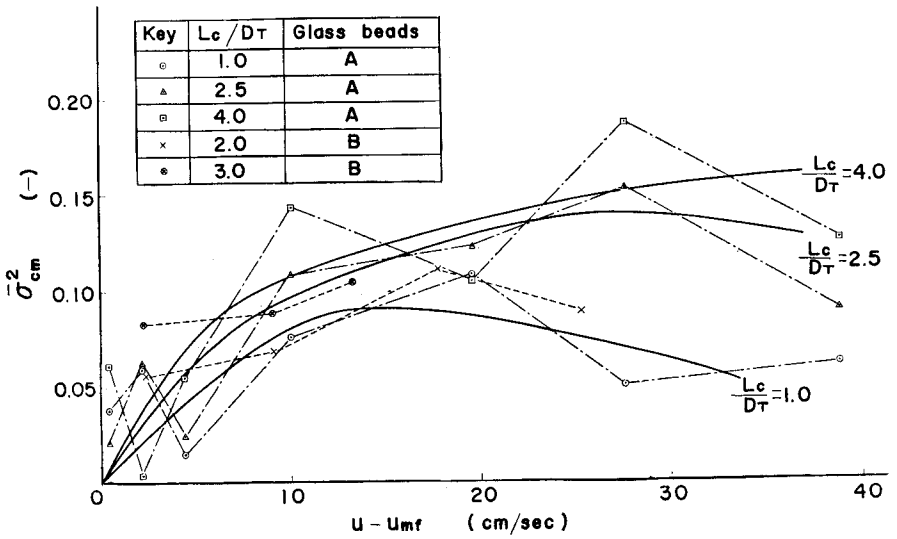

Fig. 8. Effect of excess air velocity on $\bar{\sigma}^2_{cm}$.

precision of $\bar{\sigma}^2_{cm}$ is rather poor probably because of the two variables present in Eq. (2), but it may be seen from the figure that $\bar{\sigma}^2_{cm}$ increases with the $(u-u_{mf})$ up to about 10 cm/sec and that further increase of air velocity seems to yield significant effect of L_c/D_T on $\bar{\sigma}^2_{cm}$; especially, at small bed height of $L_c/D_T=1.0$, $\bar{\sigma}^2_{cm}$ tends to decrease.

To comfirm this, a statistical technique of analysis of variance was employed: Data with glass beads A shown in Fig. 8 were analysed, regarding them as a factorially designed experiment with two factors. L_c/D_T and $(u-u_{mf})$ were chosen as

Table 2. Analysis of variance (1).

s. v.	s. s.	d. f.	m. s.	F_0
L_c/D_T	0.003102	2	0.001551	0.997
$u-u_{mf}$	0.034017	5	0.006803	4.372*
Error	0.015562	10	0.001556	
Total	0.052681	17		

F (5, 10; 0.05)=3.33
* : significant at 5% significance level.

the factors with their number of levels being 3 and 6, respectively. The result is shown in Table 2. It reveals, over the range analysed, that the effect of air velocity on $\bar{\sigma}^2_{cm}$ is statistically significant and that the effect of L_c/D_T is not detected.

It was mentioned above that the effect of L_c/D_T becomes evident at higher air velocities. Another analysis of variance was tried to verify it; the two lower

Table 3. Analysis of variance (2).

s. v.	s. s.	d. f.	m. s.	F_0
L_c/D_T	0.009057	2	0.004528	3.521$^{\Delta}$
$u-u_{mf}$	0.016109	3	0.005370	4.176$^{\Delta}$
Error	0.007718	6	0.001286	
Total	0.032884	11		

F (2,6; 0.05)=5.14 F (2,6; 0.10)=3.46 F (3,6; 0.05)=4.76 F (3,6; 0.10)=3.29
$^{\Delta}$: significant at 10% significance level.

levels of air velocity $(u-u_{mf})=0.41$ and 2.11 (cm/sec) were discarded and only the data at four higher levels were used. The result is summarized in Table 3. This demonstrates that, in the range thus limited, the effects of both factors are significant at 10 % significance level.

From these statistical analyses, it can be said that $\bar{\sigma}^2_{cm}$ is affected chiefly by the superficial air velocity and that the bed height also becomes another significant factor at higher air velocity, or, $\bar{\sigma}^2_{cm}$ increases with L_c/D_T at higher air velocity.

Concerning this, Dotson[8] reported that the additional particles in the upper part of fluidizing column had no effect on the nonuniformity in the lower part of bed. Combining this with the information obtained from the above analyses, it may be said that the additional bed height has no effect on the nonuniformity at a given bed level, but that the nonuniformity in the upper part of bed increases with the bed height.

3.2 Particle concentration in bubble and dense phases

Fig. 9 illustrates an example of particle concentration in bubble and dense

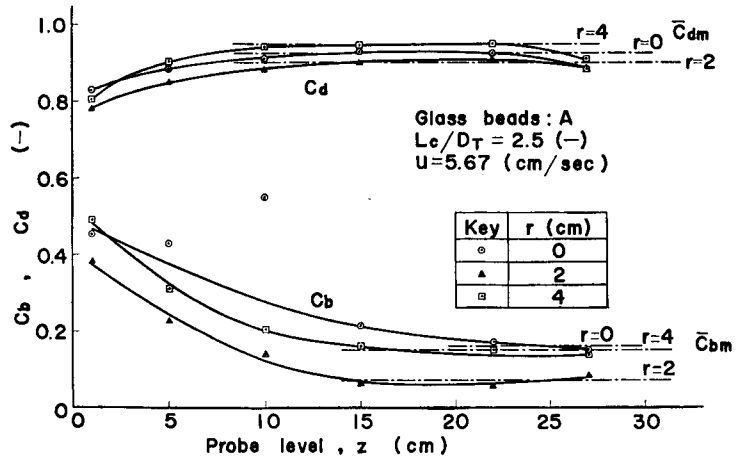

Fig. 9. An example of c_b and c_d.

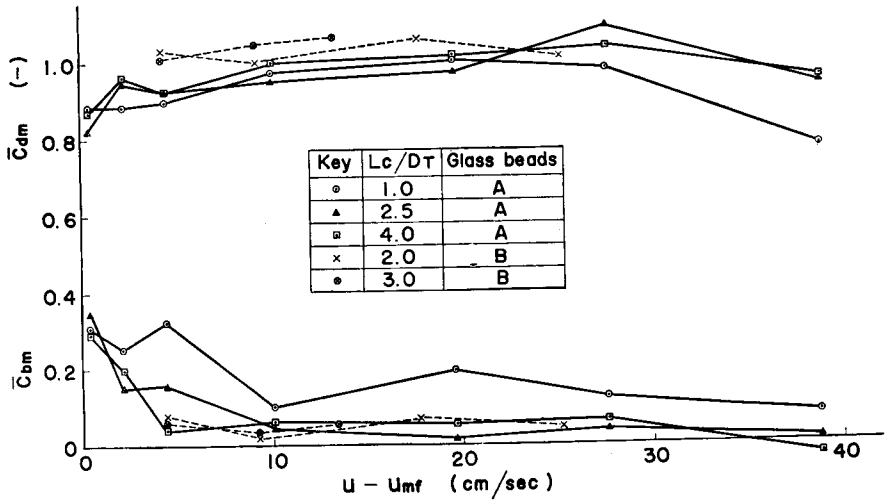

Fig. 10. Effect of excess air velocity on $\bar{c}_{bm}$ and $\bar{c}_{dm}$.

phases (c_b and c_d) in a fluidized bed of $L_c/D_T=2.5$ and $u=5.67$ cm/sec. The difference between c_b and c_d is found minor at the bottom of bed, and the difference becomes evident with increase of probe level; c_b and c_d converge to their specific values $\bar{c}_{bm}$ and $\bar{c}_{dm}$. These $\bar{c}_{bm}$ and $\bar{c}_{dm}$ are plotted in Fig. 10 against $(u-u_{mf})$. As shown in the figure, the effect of bed height and particle size on $\bar{c}_{dm}$ are not evident. Over the range studied, $\bar{c}_{dm}$ was found nearly equal to 1.0; it is very close to those measured on settled bed. In the ranges of $(u-u_{mf})$ below 2 cm/sec and above 30 cm/sec, however, $\bar{c}_{dm}$ is below 1.0. These results are so consistent with those obtained by Lanneau[9]. $\bar{c}_{bm}$ has constant value in the range of $(u-u_{mf})$ above 4 cm/sec; it is about 0.1 at $L_c/D_T=1.0$ and about 0.05 at $L_c/D_T=2.5$ and 4.0.

3.3 Rise velocity, vertical thickness and frequency of bubbles

Rise velocity of bubbles

Rise velocities of bubbles (u_b) in the fluidizing bed of $u=5.67$ cm/sec and $L_c/D_T=1.0$, 2.5 and 4.0 are summarized in Fig. 11. Though they appear dispersed owing to unknown error sources, it seems to be reasonable from this figure that the bed height has no significant effect on u_b and that the bubbles rise through the bed at a fixed velocity. Their mean ($\bar{u}_b$) are plotted against superficial air velocity in Fig. 12. From this, $\bar{u}_b$ is found to be determined by superficial air velocity and the following empirical equation can be applied.

$$\bar{u}_b=21.7\,u^{0.377} \qquad (8)$$

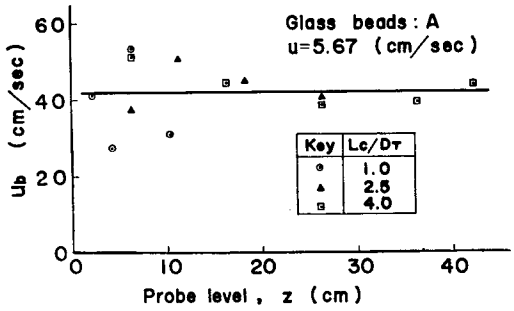

Fig. 11. Rise velocity of bubbles.

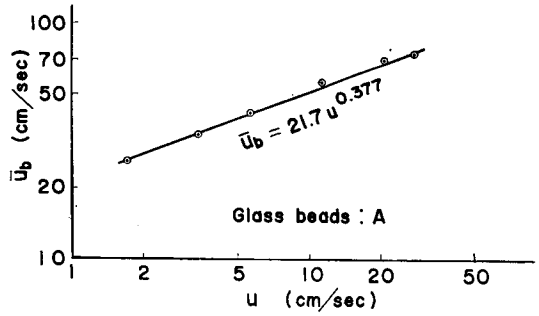

Fig. 12. Correlationship between $\bar{u}_b$ and u.

Kunii[5] and Kobayashi[10] examined the rise velocity of bubbles using cracking catalyst and silica gel as fluidized material and reported that u_b increased with the probe level. Yasui[1] reported, on the other hand, that the effect of probe level was hardly followable when glass beads or olivine was used as fluidized material and that u_b increased slightly with rising probe level when cracking catalyst was used. It may be of interest that the result of this work that u_b remains unchanged with probe level coincides with those of Yasui, also on glass beads.

Vertical thickness of bubbles

Data on vertical thickness of bubbles (y) also disperse rather widely as shown in Fig. 13. At smaller excess air velocity above the minimal fluidization, that is, $u=1.70$ and 3.40 cm/sec, y keeps almost unvaried during the passage of bubble through the bed. y tends to increase with probe level when additional air velocity is supplied. These tendencies of y are consistent with those found by Toei[4].

The correlation between u_b and y is illustrated in Fig. 14 and it is seen in this figure that u_b agrees well with the equation, $u_b=0.732\sqrt{gy}$, obtained by Toei[4].

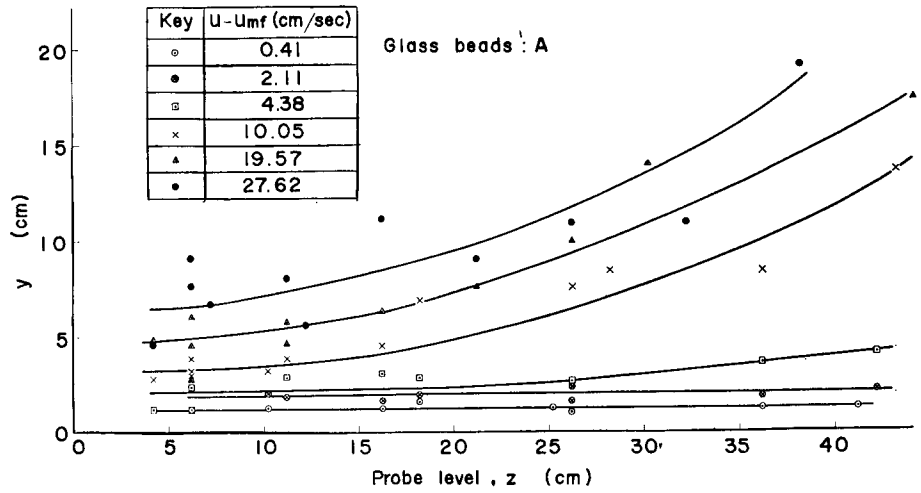

Fig. 13. Vertical thickness of bubble.

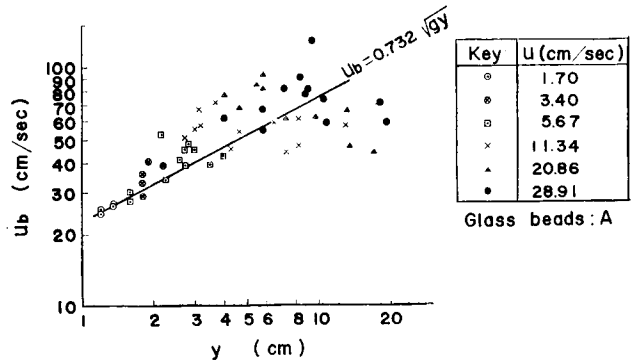

Fig. 14. Correlationship between u_b and y.

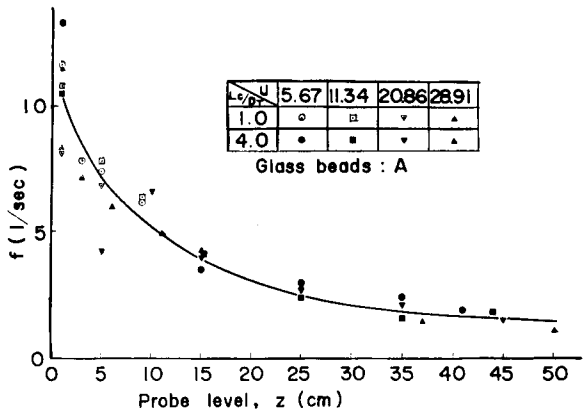

Fig. 15. Bubble frequency.

Bubble frequency

Bubble frequency (f) measured in the fluidizing bed of u=5.76, 11.34, 20.86 and 28.91 cm/sec and L_c/D_T=1.0 and 4.0 are shown in Fig. 15. Effects of bed height and air velocity on f are not detectable, and only the probel level was found affecting f over the range investigated; f decreases in raising probe level.

These tendencies of y increasing with probe level at higher air velocity and of f decreasing with probe level may be attributed to coalescing bubbles during their rise through the bed.

4. Discussion

Mean (μ_c) and variance (σ_c^2) of local particle concentration, the parameters representing fluidizing quality, were proposed and their relationship to the fluidizing conditions were mentioned. Moreover, the fluidizing characteristics such as particle concentration in bubble and dense phases (c_b and c_d), rise velocity of bubble (u_b), bubble thickness (y) and bubble frequency (f) were also measured. It is intended in this section to correlate μ_c and σ_c^2 with the fluidizing characteristics above mentioned.

μ_c defined by Eqs. (1) and (3) is expected to be a linear function composed of a product of c_b multiplied by time fraction of bubble phase covering the probe tip and another product of c_d by time fraction of dense phase covering the tip. A measure representing the former time fraction is yf/u_b, and that of the latter is $(1-yf/u_b)$.

On the other hand, σ_c^2 defined by Eqs. (2) and (4) is supposed to be zero with an uniform local particle concentration measured which is realized when only bubble phase or only dense phase covers the probe tip during the measuring time. From this, it may be presumed that σ_c^2 is a function of $(yf/u_b)(1-yf/u_b)$. In addition, σ_c^2 is also a function of difference in particle concentration between bubble and dense phases, (c_d-c_b).

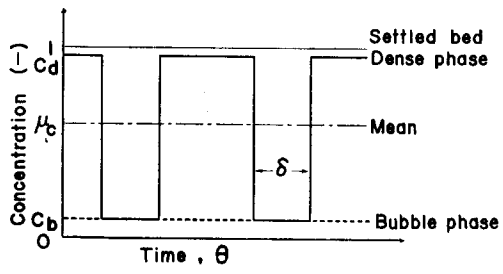

Fig. 16. Schematic oscillogram.

Keeping these characteristics of μ_c and σ_c^2 in mind, the authors[11] introduced the following equations for μ_c and σ_c^2, replacing the oscillogram of particle concentration by a rectangular wave of Fig. 16.

$$\begin{aligned}\mu_c &= \frac{1}{\theta}\int_0^{\theta} c\,d\theta \\ &= \delta f c_b + (1-\delta f)\,c_d \\ &= \frac{yf}{u_b}\,c_b + \left(1-\frac{yf}{u_b}\right)c_d \end{aligned} \tag{9}$$

$$\begin{aligned}\sigma_c^2 &= \frac{1}{\theta}\int_0^{\theta}(c-\mu_c)^2\,d\theta \\ &= \frac{1}{\theta}\int_0^{\delta f\theta}(c_b-\mu_c)^2\,d\theta + \frac{1}{\theta}\int_{\delta f\theta}^{\theta}(c_d-\mu_c)^2\,d\theta \\ &= \delta f(1-\delta f)\,(c_d-c_b)^2 \\ &= \frac{yf}{u_b}\left(1-\frac{yf}{u_b}\right)(c_d-c_b)^2 \end{aligned} \tag{10}$$

μ_c and σ_c^2 were calculated with these Eqs. (9) and (10) using measured c_b, c_d, y, u_b and f, and they were compared with measured μ_c and σ_c^2; Figs. 17 and 18 illustrate them. In Fig. 17, it is seen that the μ_c thus calculated are consistent with measured μ_c. However, σ_c^2 calculated deviates from the measured σ_c^2;

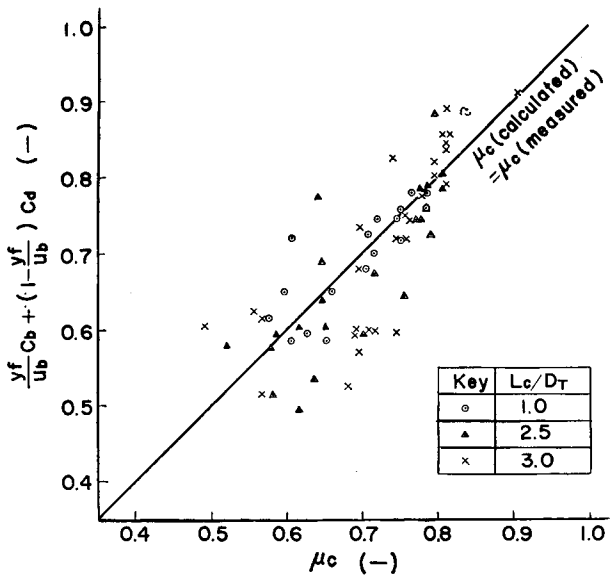

Fig. 17. Correlationship between measured and calculated μ_c.

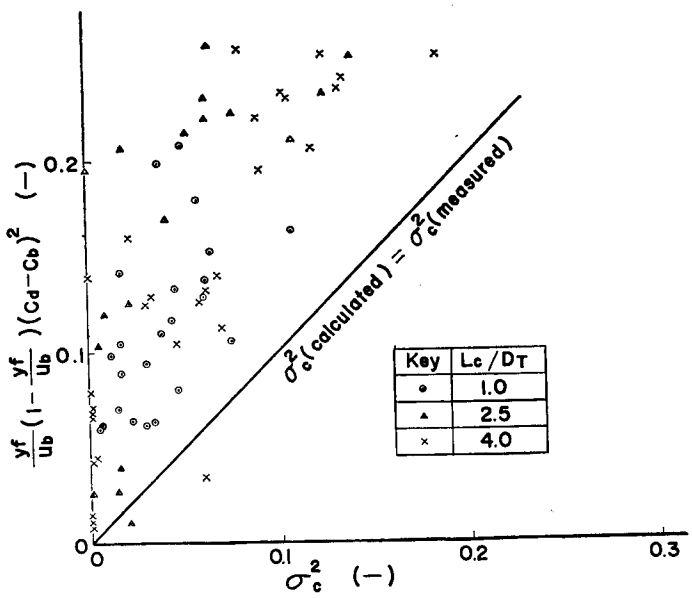

Fig. 18. Correlationship between measured and calculated σ_c^2.

calculated σ_c^2 in Fig. 18 are several times larger than the measured σ_c^2. This deviation arises from over-estimating $(c-\mu_c)^2$ in Eq. (10) in replacing the smooth oscillograms by rectangular waves. The consistency of μ_c calculated with those measured, on the other hand, are understood because both side deviations, positive and negative, of rectangular wave from the oscillogram cancel themselves.

To pursue further σ_c^2, a measure of nonuniformity, a function of c_b, c_d, y, u_b and f in the following form is presumed;

$$\sigma_c^2=A\left\{\frac{yf}{u_c}\left(1-\frac{yf}{u_b}\right)\right\}^B(c_d-c_b)^C \tag{11}$$

The constants A, B, and C in the equation are tried to be estimated by least square method; 55 sets of data on σ_c^2, c_b, c_d, y, u_b and f were applied and the resulting regression equation was,

$$\sigma_c^2=0.72\left\{\frac{yf}{u_b}\left(1-\frac{yf}{u_b}\right)\right\}^{0.46}(c_d-c_b)^{2.89} \tag{12}$$

And hence, the statistical meaning of Eq. (12) and of its exponents are to be discussed. Total sum of squares of log σ_c^2 and its degrees of freedom are,

$$\left.\begin{aligned} S_T &= \sum (\log \sigma_c^2)^2 - \frac{\{\sum (\log \sigma_c^2)\}^2}{55} = 12.4266 \\ \phi_T &= 55-1=54 \end{aligned}\right\} \quad (13)$$

Residual sum of squares from the regression and its degrees of freedom are,

$$\left.\begin{aligned} S_E &= \sum \left[\log \sigma_c^2 - \log 0.72 \left\{\frac{yf}{u_b}\left(1-\frac{yf}{u_b}\right)\right\}^{0.46} (c_d-c_b)^{2.89}\right]^2 \\ &= 8.3844 \\ \phi_E &= 55-3=52 \end{aligned}\right\} \quad (14)$$

and sum of squares due to the regression and its degrees of freedom are,

$$\left.\begin{aligned} S_R &= S_T - S_E = 4.0422 \\ \phi_R &= \phi_T - \phi_E = 54-52=2 \end{aligned}\right\} \quad (15)$$

With these, F-ratio for testing the statistical significance on the regression equation (12) is calculated as,

$$\left.\begin{aligned} F_0 &= \frac{S_R/\phi_R}{S_E/\phi_E} = 12.54^{**} \\ &\text{where} \\ F(2,52;\ 0.01) &< F(2,\ 40;\ 0.01) = 5.18 \end{aligned}\right\} \quad (16)$$

Thus, F_0 is larger than its critical value of $F(2,52;\ 0.05)$, meaning that Eq. (12) is statistically significant to represent σ_c^2.

Exponents B and C in Eq. (11) are tested as the next step; hypotheses $B=0$ and $C=0$ are tested by likelihood ratio test. Upon the hypothesis $B=0$, for example, the equation $\sigma_c^2=A(c_d-c_b)^C$ is valid instead of Eq. (11). Residual sum of squares on the hypothesis $B=0$ and its degrees of freedom are,

$$\left.\begin{aligned} S_{E(B=0)} &= \sum \left\{\log \sigma_c^2 - \log A(c_d-c_b)^C\right\}^2 \\ \phi_{E(B=0)} &= 55-2=53 \end{aligned}\right\} \quad (17)$$

Sum of squares due to term of B and its degrees of freedom are,

$$\left.\begin{aligned} S_B &= S_{E(B=0)} - S_E = 0.0847 \\ \phi_B &= \phi_{E(B=0)} - \phi_E = 1 \end{aligned}\right\} \quad (18)$$

and the F-ratio is

$$\left.\begin{aligned} F_0 &= \frac{S_B/\phi_B}{S_E/\phi_E} = 0.53 \\ &\text{where} \\ F(1,52;\ 0.05) &> F(1,60;\ 0.05) = 4.00 \end{aligned}\right\} \quad (19)$$

F_0 is less than its critical value and the hypothesis $B=0$ is not rejected at 5% significance level. Similar test of hypothesis $C=0$ was tried and it gave $F_0=21.64$. The critical value is $F(1,52;\ 0.05)<F(1,40;\ 0.05)=4.08$ and the hypothesis $C=0$ was rejected at 5% significance level. It can be said from this that the term (c_d-c_b) is indispensable to σ_c^2.

Summarizing the above statistical analyses, it is concluded that σ_c^2 represents the nonuniformity in fluidized bed mainly in terms of particle concentration difference between bubble and dense phases.

5. Summary

As a measure of nonuniformity in fluidized bed, variance (σ_c^2) of local particle concentration in the bed was proposed. In addition to this, the mean local particle concentration (μ_c) was also studied. They were measured with capacitance probe method using an integrator and a vacuum tube thermocouple. The fluidizing characteristics of the bed such as particle concentration in bubble phase (c_b) and in dense phase (c_d), rise velocity of bubble (u_b), vertical thickness of bubble (y) and bubble frequency (f) were also measured.

From the measurement on μ_c, it was found that μ_c in the bulk of bed remains at a constant value, $\overline{\mu}_{cm}$, determined by the fluidizing conditions and $\overline{\mu}_{cm}$ decreases with increasing excess air velocity above minimal fluidization. σ_c^2 increases with probe level and becomes unvaried in the upper portion of the fluidized bed. $\bar{\sigma}_{cm}^2$ in this portion increases with bed height and excess air velocity.

At the bottom of fluidizing bed, particle concentration difference between bubble and dense phases (c_d-c_b) is minor. This suggests that the bubbles are just born there and are not yet grown in their size. On rising the probe level, c_b and c_d converge to their specific values, $\bar{c}_{bm}$ and $\bar{c}_{dm}$. $\bar{c}_{dm}$ are found around 1.0, very close to those in settled bed. Regardless of the other fluidizing conditions, $\bar{c}_{bm}$ is found at about 0.1 with fluidized bed of L_c/D_T at 1.0 and at about 0.05 with that of L_c/D_T at 2.5 and 4.0.

Effects of bed height and probe level on rise velocity of bubbles (u_b) are not followable and the bubbles rise through the bed at a fixed velocity. The mean $\bar{u}_b$ is determined chiefly by air velocity and the following empirical equation was obtained.

$$\bar{u}_b=21.7u^{0.377}$$

Vertical thickness of bubble (y) increases with raising probe level at larger air velocity and bubble frequency (f) decreases with probe level. These tendencies of y and f can be attributed to the coalescence of bubbles during their rise through

the bed. Thus, the bubbles born at the bottom of fluidized bed grow up by coalesing each other in rising through the bed, mainly around its central axis. Their rising velocity is unvaried. Mean local particle concentration μ_c is well represented by c_b, c_d, y, u_b and f in the form of

$$\mu_c=\frac{yf}{u_b}c_b+\left(1-\frac{yf}{u_b}\right)c_d$$

On the other hand, σ_c^2, a measure of nonuniformity in fluidized bed, cannot be explained by Eq. (10) which assumes the rectangular waves. The regression equation of σ_c^2 is expressed by,

$$\sigma_c^2=0.72\left\{\frac{yf}{u_b}\left(1-\frac{yf}{u_b}\right)\right\}^{0.46}(c_d-c_b)^{2.89}$$

And from statistical tests on its exponents, it was found that σ_c^2 varies mainly with (c_d-c_b) term and the effect of $yf/u_b(1-yf/u_b)$ term on σ_c^2 is not significant. This concludes that σ_c^2 represents the nonuniformity in fluidized bed particularly in term of particle concentration difference between bubble and dense phases.

Acknowledgement

This work was partially supported by Scientific Research Funds provided by the Ministry of Education of Japan, for which the authors wish to express their thanks.

Symbols used

c_b	=particle concentration in bubble phase	(—)
$\bar{c}_{bm}$	=mean particle concentration in bubble phase in the upper part of bed	(—)
c_d	=particle concentration in dense phase	(—)
$\bar{c}_{dm}$	=mean particle concentration in dense phase in the bulk of bed	(—)
f	=bubble frequency	(1/sec)
u	=superficial air velocity	(cm/sec)
u_b	=rise velocity of bubble	(cm/sec)
u_{mf}	=u at minimal fluidization	(cm/sec)
v	=output D.C. signal from detector	(mV)
v_0	=v from the empty column	(mV)
v_b	=v from bubble phase	(mV)
v_d	=v from dense phase	(mV)
v_s	=v from settled bed	(mV)
y	=vertical thickness of bubble	(cm)

z	=probe level measured	(cm)
D_T	=internal diameter of fluidizing column	(cm)
L_c	=settled bed height	(cm)
S_E	=residual sum of squares	(—)
S_R	=sum of squares due to regression	(—)
S_T	=total sum of squares	(—)
δ	=width of peak on oscillogram	(sec)
θ	=time	(sec)
μ_c	=mean of particle concentration	(—)
$\overline{\mu}_{cm}$	=mean of μ_c in the bulk of bed	(—)
μ_s	=v from settled bed (=v_s)	(mV)
μ_v	=mean of v	(mV)
σ_c^2	=variance of particle concentration	(—)
$\bar{\sigma}_{cm}^2$	=mean of σ_c^2 in the upper part of bed	(—)
σ_v^2	=variance of v	(mV^2)
ϕ_E	=degrees of freedom of S_E	(—)
ϕ_R	=degrees of freedom of S_R	(—)
ϕ_T	=degrees of freedom of S_T	(—)

References

1) Yasui, G. and N.L. Johanson: Characteristics of Gas Pockets in Fluidized Beds, A. I. Ch. E. Journal, 1958, vol. 4, No. 4, 445–452
2) Harrison, D., J.F. Davidson and J.W. de Kock: On the Nature of Aggregative and Particulate Fluidization, Trans. Instn Chem. Engrs, 1961, vol. 39, 202–211
3) Baumgarten, P.K. and R.L. Pigford: Density Fluctuation in Fluidized Beds, A.I. Ch. E. Journal, 1960, vol. 6, No. 1, 115–123
4) Toei, R., R. Matsuno et al.: Behavior of Bubbles in Gas Fluidized Bed, Symposium on Chem. Eng., 1964, No. 3, 32–38
5) Hiraki, I., K. Yoshida and D. Kunii: Behaviour of Bubbles in Two-dimensional Fluidized Bed, Chem. Eng. (Japan), 1965, vol. 29, No. 11, 846–851
6) Morse, P.D. and C.D. Ballou: The Uniformity of Fluidization-Its Measurement and Use, Chem. Eng. Progr., 1951, vol. 47, No. 4, 199–204
7) Shuster, W.W. and P. Kisliak: The Measurement of Fluidization Quality, Chem. Eng. Progr., 1952, vol. 48, No. 9, 455–458
8) Dotson, J.M.: Factors Affecting Density Transients in a Fluidized Bed, A. I. Ch. E. Journal, 1959, vol. 5, No. 2, 169–174
9) Lanneau, K.P.: Gas-Solids Contacting in Fluidized Beds, Trans. Instn Chem. Engrs, 1960, vol. 38, 125–143
10) Kobayashi, H., F. Arai and T. Chiba: Behavior of Bubbles in Gas Solid Fluidized Bed, Chem. Eng. (Japan), 1965, vol. 29, No. 11, 858–863
11) Asaki, Z. and Y. Kondo: Fluctuation of Particle Concentration in Fluidized Bed, Chem. Eng. (Japan), 1965, vol. 29, No. 11, 899–900